thermo

MDPI

Article

The Optimal Design of a Heat Recovery Steam Generator Using a Thermal-Hydraulic Model

Somchart Chantasiriwan

Faculty of Engineering, Thammasat School of Engineering, Thammasat University, Pathum Thani 12121, Thailand; somchart@engr.tu.ac.th

Abstract

A heat recovery steam generator is a device used in a downstream process to recover thermal energy from the exhaust gas of an upstream system. It consists of a superheater, an evaporator, and an economizer connected in series along the direction of exhaust gas flow. The steam generated by this device may be used to produce power in a Rankine cycle. There have been several studies on the thermodynamic analysis of heat recovery steam generators, but there have been only a few thermal-hydraulic studies, despite the fact that the thermal-hydraulic behavior of this device has to be understood in order that the thermal system design can be carried out effectively. An objective of this paper is to propose an approach for thermal design of a heat recovery steam generator that considers thermodynamics, heat transfer, and fluid mechanics in its performance. This approach requires a model that characterizes a cross-flow heat exchanger in terms of its geometric parameters. It is demonstrated that these parameters can be optimized so that the total tube material cost is minimized subject to the conditions of the specified values of the net power output, the heat recovery steam generator size, and the maximum gas mass flux.

Keywords: thermal design; waste heat boiler; HRSG; optimization

1. Introduction

Waste heat in the form of hot gases occurs in several systems that use gas turbines, incinerators, cement kilns, and furnace kilns. Among various options for recovering thermal energy from hot gases, a Rankine cycle is probably the most efficient option if the gas temperature is sufficiently high. A power generation system based on a Rankine cycle consists of a waste heat boiler or a heat recovery steam generator, a steam turbine, a condenser, and auxiliary equipment. The generated power may be used internally or exported to the grid.

Heat recovery steam generators have been commonly designed using finned tubes to enhance gas-side heat transfer and minimize equipment size. This design is widely used in combined-cycle power plants that burn natural gas and produce clean flue gas. However, there are heat recovery steam generators that operate under conditions in which finned tubes may be inappropriate. These conditions exist in sulfuric acid plants, biomass combustion systems, cement industries, steel industries, and petrochemical industries because flue gas is often laden with particulate matter, corrosive species, or erosive components. Under these conditions, finned surfaces are highly susceptible to fouling, plugging, corrosion, and mechanical degradation, leading to severe performance deterioration and increased maintenance requirements. Consequently, bare or finless tubes should be used in waste heat boilers or heat recovery steam generators despite their inferior heat transfer performance compared with finned tubes.

Check for updates

Received: 16 October 2026
Revised: 20 November 2026
Accepted: 24 November 2026
Published: 28 November 2026

Copyright: © 2026 by the author. Licensee MDPI, Basel, Switzerland. This article is an open access article distributed under the terms and conditions of the Creative Commons Attribution (CC BY) license.

There have been several studies on the design and analysis of heat recovery steam generators with finned tubes [1–18]. Few studies have considered heat recovery steam generators with finless or bare tubes [13,19,20]. Each heat exchanger in a heat recovery steam generator is a cross-flow heat exchanger. A bare-tube configuration of the heat exchanger is characterized by several geometric parameters, which are the tube outer diameter and the wall thickness, the number of tube columns, the number of tube rows, the distance between centers of two nearby tubes in a row, the distance between centers of two nearby tubes in a column, and the tube length. Hence, there are a large number of configurations of the superheater, evaporator, and economizer. The design of a heat recovery steam generator should consider trade-offs among heat transfer performance, pressure drop, and operation constraints in these heat exchangers to identify the optimal geometric parameters.

Optimization of heat recovery steam generators has been a subject of several research studies. In an optimization study, one or more objective functions are defined, and one or more constraints are imposed. Objective functions may be exergy destruction [2], power production of the system [3,9], entropy generation [4,8,9], installation cost of the heat recovery steam generator [11,12], total system cost [13], exergy efficiency [13], and total exergy destruction cost [16]. Constraints may be steam quality at the turbine outlet [2], the size of the heat recovery steam generator [4,8,9,12,17], and the outlet gas temperature [13]. One of the most tangible objective functions is the total material cost of heat exchanger tubes in a heat recovery steam generator. Although there have been studies on the optimization of installation and system costs of heat recovery steam generators, the authors of most of them [11,12] were concerned with finned-tube configurations of heat recovery steam generators instead of bare-tube configurations, which are the focus of this study. Although Ghaffari et al. [13] considered bare-tube configurations, they did not optimize the geometric parameters.

The objective of this paper is to provide a procedure for the optimal thermal-hydraulic design of heat recovery steam generators with bare-tube configurations. Given the mass flow rate and temperature of a gas and the known composition of the gas at the inlet of a heat recovery steam generator, this procedure can be used to determine the optimal geometric parameters of the superheater, evaporator, and economizer that minimize the total tube material cost of the heat recovery steam generator that has a specified size in a Rankine cycle that produces a specified value of net power output.

2. Heat Recovery Steam Generator

Figure 1 shows a Rankine cycle in which the heat recovery steam generator is the heat source. The four main components of the heat recovery steam generator are the economizer (EC), evaporator (EV), steam drum (SD), and superheater (SH). The conversion of water to steam in the heat recovery steam generator occurs in three stages. The first stage is raising the water temperature in the economizer. The second stage is the water vaporization in the evaporator. The third stage is raising the steam temperature in the superheater. The pressure losses in the three heat exchangers are denoted by Δp_{EC}, Δp_{EV}, and Δp_{SH}. Hot gas flows successively through the superheater, evaporator, and economizer before being exhausted to the surroundings. Its temperature decreases from T_{g1} to T_{g4}. Its pressure decreases from the ambient pressure (p_a) to the exhaust pressure ($p_a - \Delta p_g$).

Water leaving the condenser (C) is saturated liquid with a mass flow rate of m_s and an enthalpy of h_{lc}. A pump is used to increase the water pressure from p_c to $p_s + \Delta p_{SH} + \Delta p_{EC}$ before the water enters the economizer. The pump work input is given by Equation (1).

$$w_p = \frac{v_c(p_s + \Delta p_{SH} + \Delta p_{EC} - p_c)}{\eta_{pump}} \quad (1)$$

where v_c is the specific volume of liquid water at pressure p_c, and η_{pump} is the pump efficiency. The enthalpy h_w at the economizer inlet is determined as follows:

$$h_w = h_{lc} + w_p \tag{2}$$

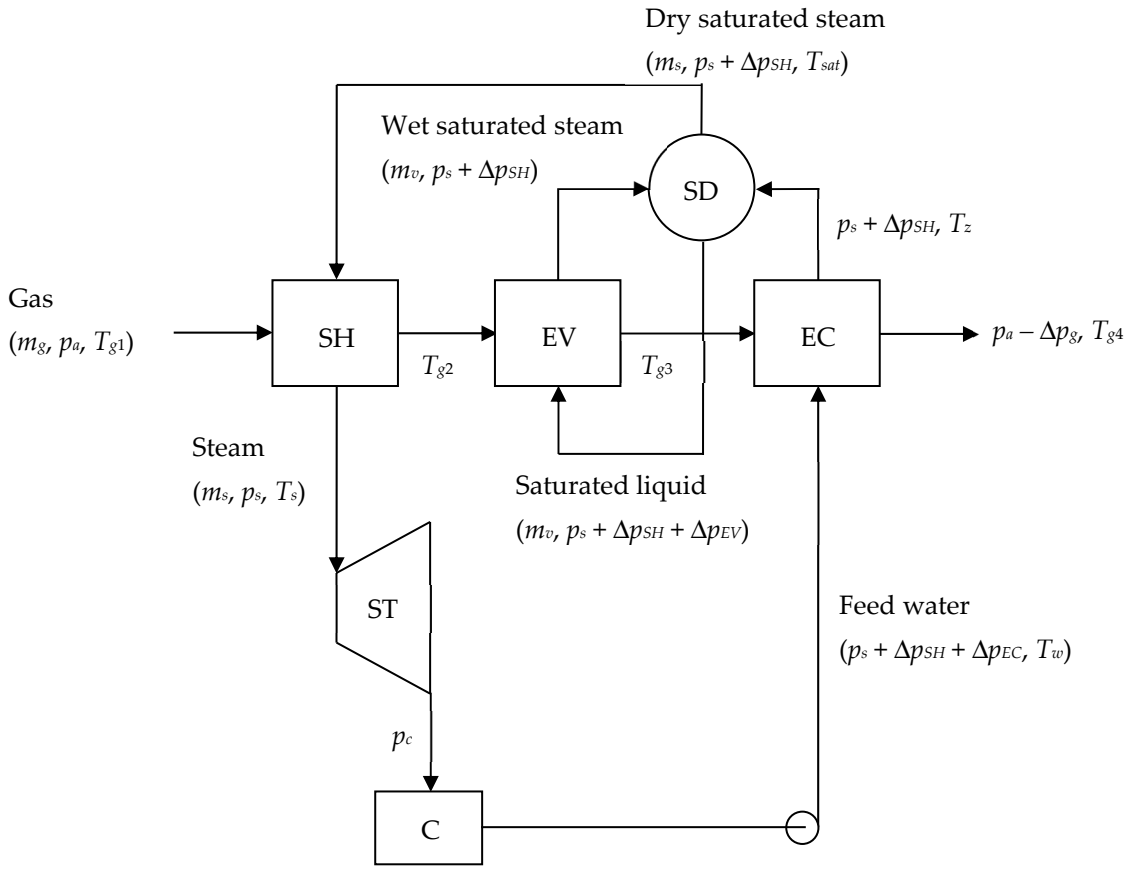

Figure 1. Heat recovery steam generator in Rankine cycle.

Heating in the economizer raises the water temperature from T_w to T_z, which is less than the saturation temperature (T_{sat}). The water pressure at the economizer outlet is $p_s + \Delta p_{SH}$. The steam drum pressure is also $p_s + \Delta p_{SH}$. Inside the steam drum, the subcooled feed water from the economizer is mixed with the wet saturated steam from the evaporator. Dry saturated steam and saturated liquid water are separated in the steam drum. The saturated liquid is returned to the evaporator, whereas the dry saturated steam is sent to the superheater. It should be noted that tubes carrying water from the steam drum to the evaporator are not in the gas flow path as shown in Figure 1. A more accurate illustration must be drawn in three dimensions that will show these tubes in a different plane.

It is assumed that the steam drum is located at an elevation that permits steam and water to circulate between the steam drum and the evaporator without a pump. Therefore, the water pressure at the evaporator inlet can be set to $p_s + \Delta p_{SH} + \Delta p_{EV}$. Vaporization in the evaporator is incomplete, and the output of the evaporator is wet saturated steam with a quality of x_{EV}. Because T_z is less than T_{sat}, the steam flow rate in the evaporator (m_v) is higher than m_s.

$$m_v = \frac{m_s}{x_{EV}} \left(\frac{h_v - h_z}{h_v - h_l} \right) \tag{3}$$

where h_v and h_l are the enthalpies of saturated vapor and saturated liquid at the steam drum pressure. In this study, it is assumed that x_{EV} is 0.1. After leaving the superheater, the steam temperature is increased to T_s, and the steam pressure is decreased to p_s.

Steam from the superheater expands in the steam turbine (ST), and its pressure is reduced from p_s to p_c. The resulting power output of the steam turbine is given by Equation (4).

$$P_{out} = m_s \eta_{turbine} (h_s - h_{cs}) \tag{4}$$

where h_s is the specific enthalpy of the steam, h_{cs} is the specific enthalpy after isentropic expansion from p_s to p_c, and $\eta_{turbine}$ is the turbine efficiency. The gross power output is the difference between the turbine power output and the pump power input.

$$P_{gross} = P_{out} - m_s w_p \tag{5}$$

The fan power required for the gas flow through the heat recovery steam generator is given by Equation (6).

$$P_{fan} = \frac{m_g v_g \Delta p_g}{\eta_{fan}} \tag{6}$$

where v_g is the specific volume of the gas, and η_{fan} is the fan efficiency. The net power output is the difference between the gross power output and the fan power.

$$P_{net} = P_{gross} - P_{fan} \tag{7}$$

Models of heat recovery steam generators may be divided into black-box models [21–23], thermodynamic models [24–29], and thermal-hydraulic models [3,4,11–13]. A heat recovery steam generator is viewed as a single unit in black-box models. In both thermodynamic and thermal-hydraulic models, components of a heat recovery steam generator are considered separately. Equations of energy balances of the superheater, evaporator, and economizer are given by Equations (8)–(10).

$$m_g c_{pg} (T_{g1} - T_{g2}) = m_s (h_s - h_v) \tag{8}$$

$$m_g c_{pg} (T_{g2} - T_{g3}) = m_s (h_v - h_z) \tag{9}$$

$$m_g c_{pg} (T_{g3} - T_{g4}) = m_s (h_z - h_w) \tag{10}$$

The performance of a heat recovery steam generator depends on its total heating surface area, which is the sum of the heating surface areas of the superheater, evaporator, and economizer. For each heat exchanger, the relationships among the fluid temperatures, flow rates, and heating surface area may be determined by using the effectiveness-NTU method. Let Q denote the rate of heat transfer from the hot fluid to the cold fluid in the heat exchanger; the capacity rates of the gas (C_h) and the steam or water (C_c) are defined in Equations (11) and (12).

$$C_c = m_c c_{pc} \tag{11}$$

$$C_h = m_h c_{ph} \tag{12}$$

where m_c and m_h are the mass flow rates of the cold and hot fluids, and c_{pc} and c_{ph} are the specific heat capacities of the cold and hot fluids. The cold fluid is the steam or water, whereas the hot fluid is the gas. The lower value of capacity rates is C_{min}, and the higher value is C_{max}. In the superheater and economizer, C_{min} is C_c because the gas flow rate is much larger than the steam or water flow rate. In the evaporator, C_c is treated as infinite because of the unchanging temperature of the cold fluid during vaporization, and C_{min} is C_h.

The ratio of capacity rates, the number of transfer units, and the heat exchanger effectiveness are defined as follows:

$$c = \frac{C_{min}}{C_{max}} \tag{13}$$

$$NTU = \frac{UA}{C_{min}} \tag{14}$$

$$\varepsilon = \frac{Q}{C_{min}(T_{hi} - T_{ci})} \tag{15}$$

where U is the overall heat transfer coefficient, A is the heating surface area, T_{hi} is the inlet temperature of the hot fluid, and T_{ci} is the inlet temperature of the cold fluid. Each heat exchanger in a heat recovery steam generator may be modeled as a single-pass or a multi-pass cross-flow heat exchanger with cold fluid unmixed and hot fluid mixed.

Consider a cross-flow heat exchanger with n passes. Let the heating surface area of 1 pass be A_1. The number of transfer units corresponding to this area is expressed as

$$NTU_1 = \frac{UA_1}{C_{min}} \tag{16}$$

The effectiveness of a one-pass cross-flow heat exchanger with cold fluid unmixed and hot fluid mixed is given by the following function of NTU_1 and c.

$$\varepsilon_1 = \frac{1}{c}\left[1 - e^{-c(1-e^{-NTU_1})}\right] \tag{17}$$

It was shown by Dhar [30] that the effectiveness of a cross-flow heat exchanger with n passes is given by Equation (18).

$$\varepsilon = \frac{\left(\frac{1-\varepsilon_1}{1-c\varepsilon_1}\right)^n - 1}{c\left(\frac{1-\varepsilon_1}{1-c\varepsilon_1}\right)^n - 1} \tag{18}$$

In an evaporator, c is zero, and

$$\varepsilon = 1 - e^{-NTU} \tag{19}$$

The difference between thermodynamic and thermal-hydraulic models lies in how overall heat transfer coefficients of the superheater, evaporator, and economizer are determined. Empirical correlations are used to compute overall heat transfer coefficients without knowledge of geometric parameters in thermodynamic models. In thermal-hydraulic models, each heat exchanger in a heat recovery steam generator is modeled as a cross-flow heat exchanger. The overall heat transfer coefficient depends on the geometric parameters of the heat exchanger.

3. Cross-Flow Heat Exchanger

An illustration of a cross-flow heat exchanger is shown in Figure 2. Steam or water flows inside tubes, and gas flows across them. The inner and outer diameters of each tube are D_i and D_o, and the tube length is l. Only inline arrangements of tubes are considered in this study because they offer better performance than staggered arrangements according to a previous study [13].

The heat exchanger consists of N_c columns of tubes in a plane that is perpendicular to the gas flow direction. The distance between the centers of adjacent tubes in this plane is the transverse tube pitch (S_T). There are N_r rows of tubes in a plane that is parallel to the gas flow direction. The distance between the centers of adjacent tubes in this plane is the longitudinal tube pitch (S_L). It is usual to specify tube pitch ratios (S_T/D_o and S_L/D_o) instead of tube pitches. The cross-flow heat exchanger shown in Figure 2 represents the superheater, evaporator, or economizer. In the superheater or economizer, steam or water flows through N_c tube circuits. Each circuit is formed by connecting two adjacent tubes in a plane that is parallel to the gas flow direction with a 180° elbow. In the evaporator, there are N_cN_r tubes. Saturated liquid flows upward in each tube and becomes saturated steam at the tube outlet.

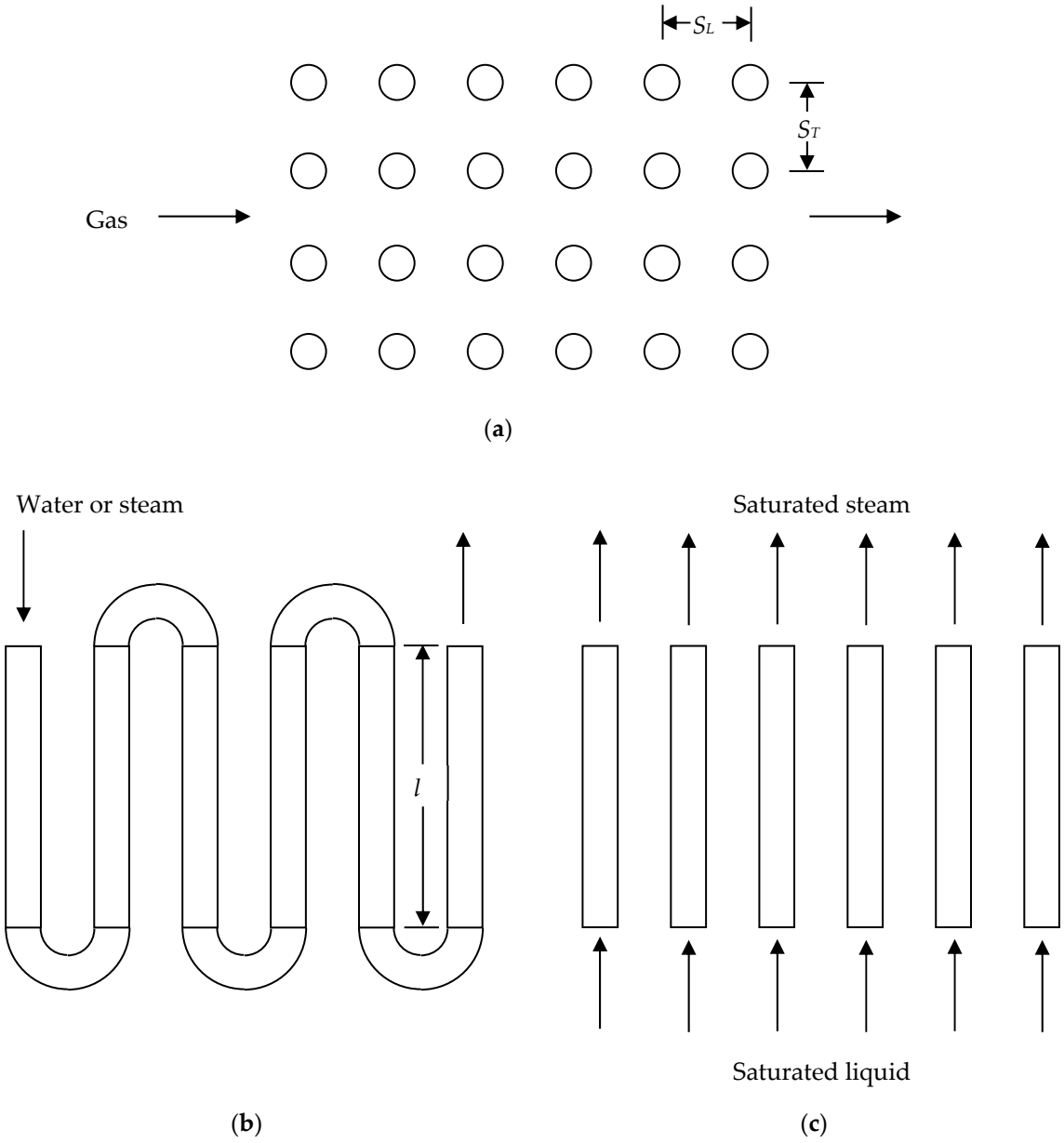

Figure 2. Geometry of the superheater, evaporator, or economizer: (**a**) top view, (**b**) side view of the superheater or economizer, and (**c**) side view of the evaporator.

In general, there are three sets of geometric parameters (N_c, N_r, S_T, S_L, D_i, D_o, and l) for the superheater, evaporator, and economizer. A constraint may be imposed so that all three heat exchangers have the same tube diameters (D_i and D_o) and tube length (l). Furthermore, the square pitch is assumed so that S_L and S_T are equal. Therefore, the geometry of the heat recovery steam generator is defined by 12 parameters: D_i, D_o, l, N_{c1}, N_{r1}, S_{T1}, N_{c2}, N_{r2}, S_{T2}, N_{c3}, N_{r3}, and S_{T3}. Subscripts 1, 2, and 3 denote the superheater, evaporator, and economizer, respectively.

The overall heat transfer coefficient (U) based on the outer surface area is determined from the thermal resistance network.

$$\frac{1}{U} = \frac{1}{\overline{h}_o} + ff_o + \frac{D_o \ln(D_o/D_i)}{2k_w} + \frac{D_o}{D_i \overline{h}_i} \tag{20}$$

where k_w is the thermal conductivity of the tube material, $\overline{h}_i$ is the heat transfer coefficient between the inner tube surface and the steam or water, $\overline{h}_o$ is the heat transfer coefficient

between the gas and the outer tube surface, and ff_o is the fouling factor on the outer tube surface. It is assumed that the fouling factor on the inner tube surface is negligible. Radiation heat transfer is also ignored because it is much less than forced convection heat transfer.

The mass flow rate in each tube of the superheater or economizer is m_s/N_c, and the average velocity in each tube is given by Equation (21).

$$V_s = \frac{4m_s}{\pi N_c \rho_s D_i^2} \tag{21}$$

where ρ_s is the density of steam or water. Reynolds number due to steam or water flow is given by Equation (22).

$$Re_i = \frac{\rho_s V_s D_i}{\mu_s} \tag{22}$$

where μ_s is the dynamic viscosity of water or steam. The friction factor for turbulent flow inside a tube can be computed using the formula presented by Chen [31].

$$f_i = \left\{-2\log\left[\frac{e}{3.7065D_i} - \frac{5.0452}{Re_i}\log\left(\frac{(e/D_i)^{1.1098}}{2.8257} + \frac{5.8506}{Re_i^{0.8981}}\right)\right]\right\}^{-2} \tag{23}$$

where e is the roughness of the tube's inner surface.

The heat transfer coefficient inside tubes of the superheater and economizer may be determined using the correlation proposed by Gnielinski [32].

$$\frac{\bar{h}_i D_i}{k_s} = \frac{0.125 f_i (Re_i - 1000) Pr_s}{1 + 4.49\sqrt{f_i}\left(Pr_s^{2/3} - 1\right)} \tag{24}$$

where k_s and Pr_s are the thermal conductivity and Prandtl number of the water or steam flowing inside the tubes. Properties of steam or water in Equations (21)–(24) are evaluated at the average of inlet and outlet temperatures of the steam or water. According to Ganapathy [33], the inner heat transfer coefficient for the evaporator is given by Equation (25).

$$\bar{h}_i = 44.44\sqrt{q}\exp\left(\frac{p_s}{8.69}\right) \tag{25}$$

where q is heat flux, measured in W/m^2, and p_s is steam pressure, measured in MPa.

Flow through the tubes causes a pressure drop (Δp_i). Four components of pressure drop are friction loss (Δp_f), minor losses (Δp_m). elevation loss (Δp_e), and acceleration loss (Δp_a).

$$\Delta p_i = \Delta p_f + \Delta p_m + \Delta p_e + \Delta p_a \tag{26}$$

Friction loss occurs along the length of the tube.

$$\Delta p_f = \frac{f_i N_r l \rho_s V_s^2}{2D_i} \tag{27}$$

Minor losses occur at the tube entrance, tube exit, and elbows. In the superheater and economizer, there are $N_r - 1$ elbows. Therefore,

$$\Delta p_m = \left[K_{in} + K_{out} + f_i(N_r - 1)\frac{l_e}{D_i}\right]\frac{\rho_s V_s^2}{2} \tag{28}$$

where K_{in} and K_{out} are coefficients of minor losses for the tube entrance and exit, and l_e is the equivalent length of a 180° elbow. In the evaporator, there are no elbows. Consequently,

$$\Delta p_m = (K_{in} + K_{out})\frac{\rho_s V_s^2}{2} \tag{29}$$

A homogeneous model is used to determine the pressure drop in the evaporator. Therefore, ρ_s is the average of the densities of saturated steam and saturated liquid.

Elevation loss occurs when the tube outlet is higher than the tube inlet. For the superheater and economizer, it is assumed that N_r is an even number so that Δp_e is zero. For the evaporator, the elevation loss is given by Equation (30).

$$\Delta p_e = \rho_s g l \tag{30}$$

Acceleration loss occurs when the fluid velocity at the tube exit is greater than at the entrance.

$$\Delta p_a = \left(\frac{4m_s}{N_c \pi D_i^2}\right)^2 \left(\frac{1}{\rho_{out}} - \frac{1}{\rho_{in}}\right) \tag{31}$$

where ρ_{out} and ρ_{in} are the fluid densities at the exit and entrance.

The outer heat transfer coefficient is determined from the correlation suggested by Ganapathy [33].

$$\frac{\bar{h}_o D_o}{k_g} = 0.33 Re_o^{0.6} Pr_g^{0.33} \tag{32}$$

where k_g and Pr_g are the thermal conductivity and Prandtl number of the gas. Reynolds number for gas flow is given by Equation (33).

$$Re_o = \frac{G_g D_o}{\mu_g} \tag{33}$$

where μ_g is the dynamic viscosity of the gas, and G_g is the gas mass flux.

$$G_g = \frac{m_g}{N_c l (S_T - D_o)} \tag{34}$$

The gas properties in Equations (32)–(34) are evaluated at the average of the inlet and outlet temperatures of the gas.

Gas flow across the tube bank results in the following pressure drop [33].

$$\Delta p_o = \frac{0.204 N_r f_o G_g^2}{\rho_g} \tag{35}$$

where ρ_g is the gas density. The friction factor can be computed as follows:

$$f_o = Re_o^{-0.15}\left[0.044 + \frac{0.08 S_L}{D_o (S_T/D_o - 1)^{(0.43 + 1.13 D_o/S_L)}}\right] \tag{36}$$

The total gas pressure drop is the difference between the gas pressures at the inlet and outlet of the heat recovery steam generator. It is the sum of the pressure drops across the superheater, evaporator, and economizer tube banks.

$$\Delta p_g = \Delta p_{o,SH} + \Delta p_{o,EV} + \Delta p_{o,EC} \tag{37}$$

4. Optimization Procedure

In a practical design of a heat recovery steam generator, it is usual to specify the net power output (P_{net}). It is interesting to note that the individual tube length (l) is approximately the height of the heat recovery steam generator. Therefore, it represents the size of the heat recovery steam generator. The objective in this study is to determine the geometric parameters for the construction of a heat recovery steam generator of a specified size that will deliver the specified net power output. Since there are many different sets of possible geometric parameters, the optimal set should be the one that results in the

minimum material cost. Therefore, the optimization procedure in this study is used to minimize the total material cost subject to the specified values of the net power output and the individual tube length.

Assume that m_g, T_{g1}, p_s, p_c, D_i, D_o, l, N_{c1}, N_{r1}, N_{c2}, N_{r2}, N_{c3}, and N_{r3} are known. By imposing the identical design value of mass flux (G_{gd}) across the tube banks of the superheater, evaporator, and economizer, S_{T1}, S_{T2}, and S_{T3} are determined as follows.

$$S_{T1} = D_o + \frac{m_g}{N_{c1} l G_{gd}} \tag{38}$$

$$S_{T2} = D_o + \frac{m_g}{N_{c2} l G_{gd}} \tag{39}$$

$$S_{T3} = D_o + \frac{m_g}{N_{c3} l G_{gd}} \tag{40}$$

The steam flow rate (m_s), steam temperature (T_s), the water temperature at the economizer outlet (T_z), and pressure drops in the superheater and economizer tubes (Δp_{SH} and Δp_{EC}) can be determined by using the iteration procedure shown in Figure 3. An initial value of m_s is required to calculate U_{SH}, U_{EV}, and U_{EC} using Equation (20).

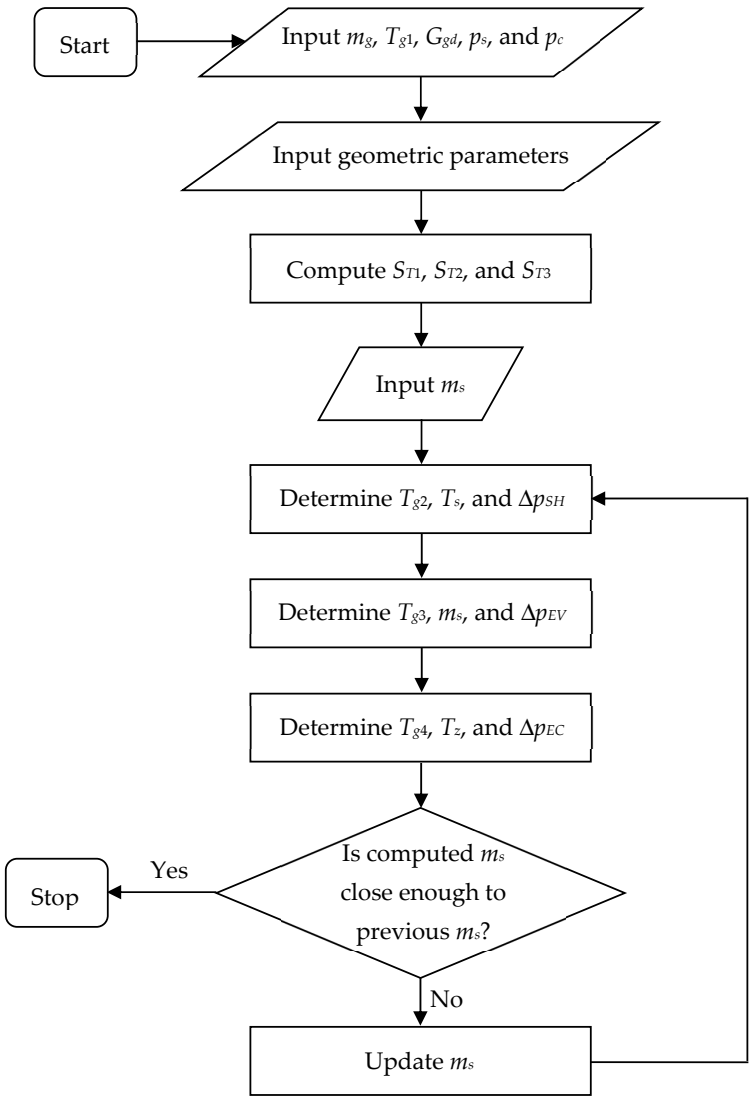

Figure 3. Flow chart for the simulation of a heat recovery steam generator.

If m_g, T_{g1}, and p_c are fixed parameters, P_{net} depends on p_s, G_{gd}, l, and the other geometric parameters. Consequently, G_{gd} can be found for specified values of p_s, P_{net}, l, and the other geometric parameters.

For each heat exchanger, the total tube length is the product of the individual tube length and the number of tubes. Therefore, the total tube lengths of the superheater, evaporator, and economizer are given by Equations (41)–(43).

$$L_{SH} = N_{c1}N_{r1}l \tag{41}$$

$$L_{EV} = N_{c2}N_{r2}l \tag{42}$$

$$L_{EC} = N_{c3}N_{r3}l \tag{43}$$

It may be assumed that the material cost of a component of a heat recovery steam generator is proportional to the total tube length of the component. The material for the evaporator and economizer tubes is carbon steel. For the superheater tubes, low alloy steel is used because of high tube temperature. Adjusted total tube length is defined as follows:

$$L_{atot} = rL_{SH} + L_{EV} + L_{EC} \tag{44}$$

where r is the ratio of the unit cost of low alloy steel tube to that of carbon steel tube. L_{atot} is an economic parameter because the total material cost is simply the product of L_{atot} and the unit cost of carbon steel tube. It can be expressed as a function of p_s, P_{net}, l, and the other geometric parameters.

If p_s, P_{net}, and l are kept unchanged, L_{atot} can be minimized by finding optimal values of the geometric parameters. Grid search is used for this purpose. The search region in this paper is selected from typical steam and water velocities in the superheater and economizer under the assumption that too large or too small steam and water velocities are unlikely to result in the global minimum. By imposing reasonable velocities of steam and water, the numbers of tube columns and rows can be approximately determined for the superheater, evaporator, and economizer. A search region is constructed from lower and upper limits of the numbers of tube columns and rows. Grid search is then carried out to find the optimal grid point. The optimal grid point should not be too close to the search boundary. Otherwise, the search boundary near the optimal grid point has to be expanded, and the optimal grid point is searched for again. The optimization procedure continues until the optimal grid point is located near the center of the search region. The value of L_{atot} at the optimal grid point is the minimum adjusted total tube length (L_{min}), which is a function of p_s, P_{net}, and l.

5. Results and Discussion

Fortran codes were written to obtain simulation results. Gas properties were calculated using correlations provided by NIST Chemistry WebBook [34]. Water and steam thermodynamic properties were calculated according to IAPWS industrial formulation 1997 [35]. Viscosity and thermal conductivity of water or steam were calculated using methods provided by Sengers and Kamgar-Parsi [36] and Sengers et al. [37].

The thermal-hydraulic model was validated by comparing simulation results of this model with the performance data of the heat recovery steam generator reported by Ganapathy [33]. The control parameters of this model that were set equal to the corresponding parameters of the performance data are the gas flow rate and inlet temperature (m_g and T_{g1}), the steam pressure (p_s), the water temperature at economizer inlet (T_w), the outer and inner tube diameters of superheater (D_{o1} and D_{i1}), evaporator (D_{o2} and D_{i2}), and economizer (D_{o3} and D_{i3}), the transverse pitches (S_{T1}, S_{T2}, and S_{T3}), the longitudinal pitches (S_{L1}, S_{L2}, and S_{L3}), and the individual tube lengths (l_1, l_2, and l_3). The values of the control

parameters are m_g = 41.67 kg/s, T_{g1} = 650 °C, p_s = 4.1 MPa, T_w = 105 °C, D_{o1} = 31.8 mm, D_{i1} = 25 mm, $D_{o2} = D_{o3}$ = 50.8 mm, $D_{i2} = Di3$ = 44 mm, $S_{T1} = S_{T2}$ = 100 mm, S_{T3} = 90 mm, $S_{L1} = S_{L2} = S_{L3}$ = 80 mm, l_1 = 2 m, $l_2 = l_3$ = 4 m, N_{c1} = 36, N_{r1} = 6, N_{c2} = 60, N_{r2} = 20, N_{c3} = 20, and N_{r3} = 24. The control parameters were used as the input parameters of the model to determine the steam flow rate (m_s), the steam temperature (T_s), the saturation temperature (T_{sat}), the water temperature at the economizer outlet (T_z), the gas temperatures at the outlets of the superheater, evaporator, and economizer (T_{g2}, T_{g3}, and T_{g4}), the pressure losses in the superheater and economizer (Δp_{SH} and Δp_{EC}), and the total gas pressure drop (Δp_g). Table 1 shows that there is good agreement between the simulation results and the performance data.

Table 1. Comparison of simulation results and performance data [33] of a heat recovery steam generator.

Parameter	Simulation Results	Performance Data
m_s (kg/s)	7.74	7.69
T_s (°C)	319	316
T_{sat} (°C)	253	252
T_z (°C)	217	221
T_{g2} (°C)	618	619
T_{g3} (°C)	325	330
T_{g4} (°C)	245	247
Δp_{SH} (kPa)	98	86
Δp_{EC} (kPa)	17	21
Δp_g (kPa)	0.081	0.086

The thermal-hydraulic model of the heat recovery steam generator was used to simulate an optimized heat recovery steam generator integrated into a Rankine cycle. The optimization sought the minimum adjusted total tube length for a specified net power output. Table 2 shows system parameters that were unchanged during the simulation.

Table 2. System parameters.

Gas molar composition	
- N_2	73.98%
- O_2	11.28%
- CO_2	4.31%
- Ar	0.89%
- H_2O	9.54%
Gas flow rate	200 kg/s
Gas inlet temperature	580 °C
Pump efficiency	80%
Turbine efficiency	85%
Fan efficiency	85%
Condenser pressure	10 kPa
Net power output	30 MW

The superheater tubes are made of low alloy steel, whereas the evaporator and economizer tubes are made of carbon steel. The ratio of the unit cost of low alloy steel tube to that of carbon steel tube is 1.5. The outer and inner tube diameters are 4.83 cm and 4.094 cm. The specified values of p_s, P_{net}, and l are 6.0 MPa, 30 MW and 9 m. The search region is defined as follows:

- First, $70 \leq N_{c1} \leq 110$, and $6 \leq N_{r1} \leq 24$;

- Second, $60 \leq N_{c2} \leq 100$, and $17 \leq N_{r2} \leq 62$;
- Third, $20 \leq N_{c3} \leq 30$, and $100 \leq N_{r3} \leq 145$.

The grid search results are shown in Figures 4–6. It can be seen that G_{gd} increases as the number of tube columns or tube rows decreases, and L_{atot} decreases with the number of tube columns and tube rows. Decreasing N_{c1}, N_{c2}, or N_{c3} causes G_{gd} to increase according to Equation (34). Increasing G_{gd} results in increased overall heat transfer coefficient, which leads to decreasing heat transfer area and adjusted total tube length. Decreasing N_{r1}, N_{r2}, or N_{r3} causes the heating surface area of the superheater, evaporator, or economizer and L_{atot} to decrease. The overall heat transfer coefficient has to be increased to maintain the same heat transfer capacity required to generate the net power output of 30 MW, which results in increasing G_{gd}. The optimal numbers of tube columns and tube rows may be found by drawing a line of constant $G_{gd} = 12.5$ kg/m^2.s on Figures 4a and 5a, or 6a and locating the optimal grid point that has the minimum L_{atot} on this line. The optimal geometric parameters are $N_{c1} = 95$, $N_{r1} = 10$, $N_{c2} = 87$, $N_{r2} = 20$, $N_{c3} = 26$, and $N_{r3} = 112$. The minimum adjusted total tube length (L_{min}) is 54,693 m.

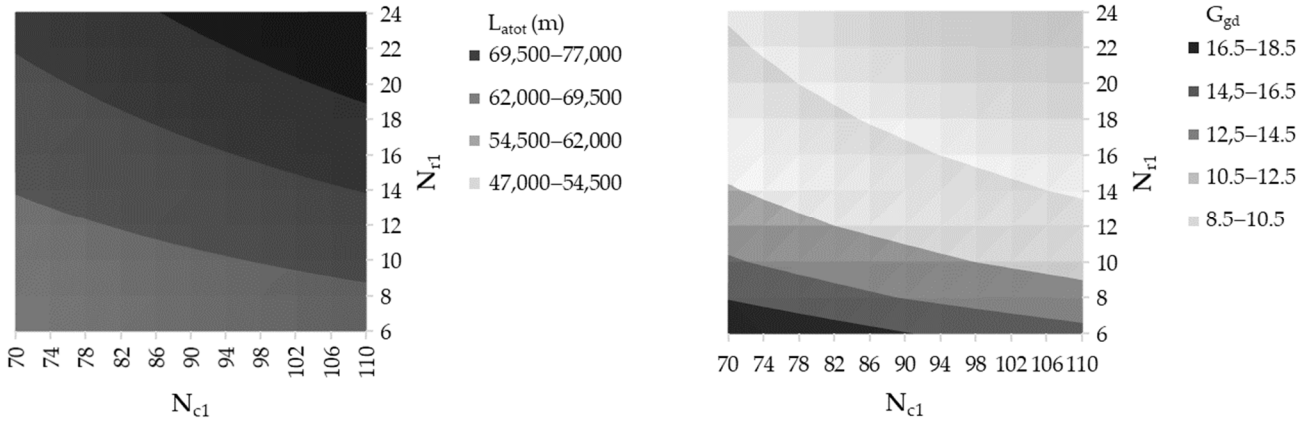

(**a**) (**b**)

Figure 4. Variations with the number of tube columns (N_{c1}) and rows (N_{r1}) in the superheater of (**a**) adjusted total tube length of heat recovery steam generator (L_{atot}) and (**b**) mass flux of gas (G_{gd}).

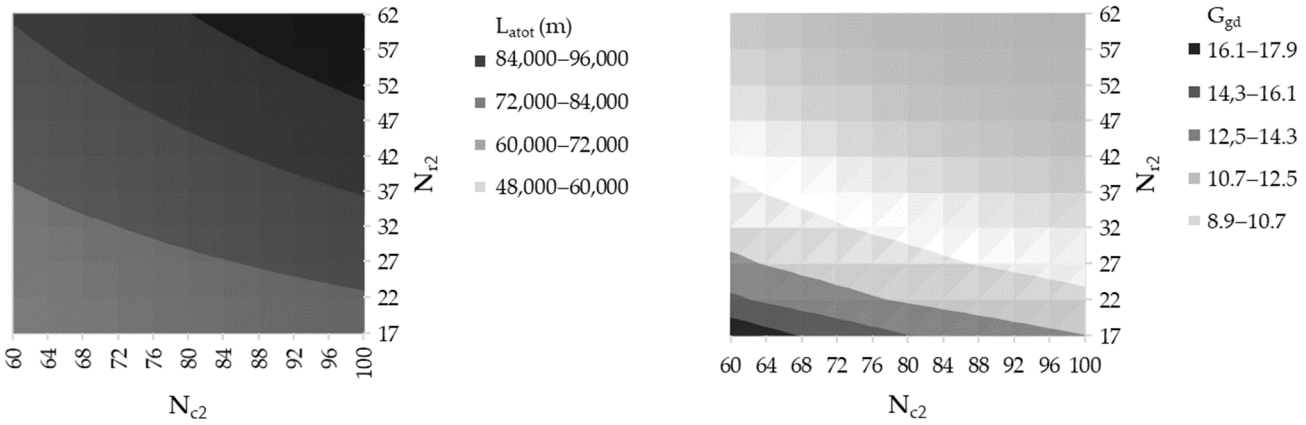

(**a**) (**b**)

Figure 5. Variations with the number of tube columns (N_{c2}) and rows (N_{r2}) in the evaporator of (**a**) adjusted total tube length of heat recovery steam generator (L_{atot}) and (**b**) mass flux of gas (G_{gd}).

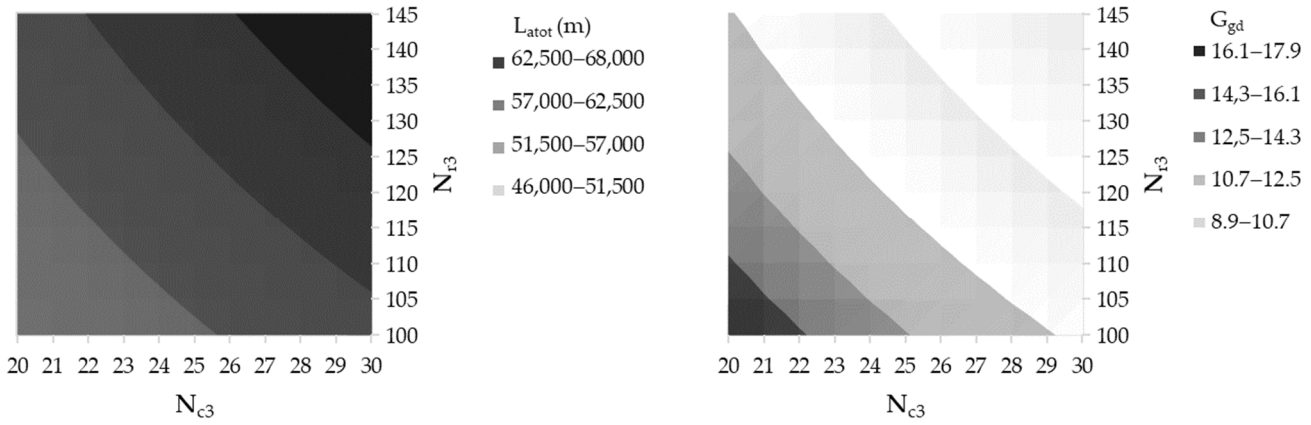

(**a**) (**b**)

Figure 6. Variations with the number of tube columns (N_{c3}) and rows (N_{r3}) in the economizer of (**a**) adjusted total tube length of heat recovery steam generator (L_{atot}) and (**b**) mass flux of gas (G_{gd}).

By changing p_s without changing l, results showing the effects of p_s were obtained. Figure 7 shows variation in L_{min} with p_s. It can be seen that L_{min} decreases from 57,285 m to 54,693 m as p_s increases from 4.0 MPa to 6.0 MPa, and increases from 54,702 m to 55,845 m as p_s increases from 7.0 MPa to 9.0 MPa. It is conceivable that the optimal p_s is between 6 MPa and 7 MPa. Additional results were obtained in this pressure range, and it was found that the minimum value of L_{min} is 54,639 at 6.5 MPa. It is interesting to note that previous studies on thermal-hydraulic models of heat recovery steam generators overlooked the dependence of optimized steam parameters on geometric parameters [4,5,11,12]. It was demonstrated in this study that the optimized steam pressure depends on optimized geometric parameters, as shown in Figure 7.

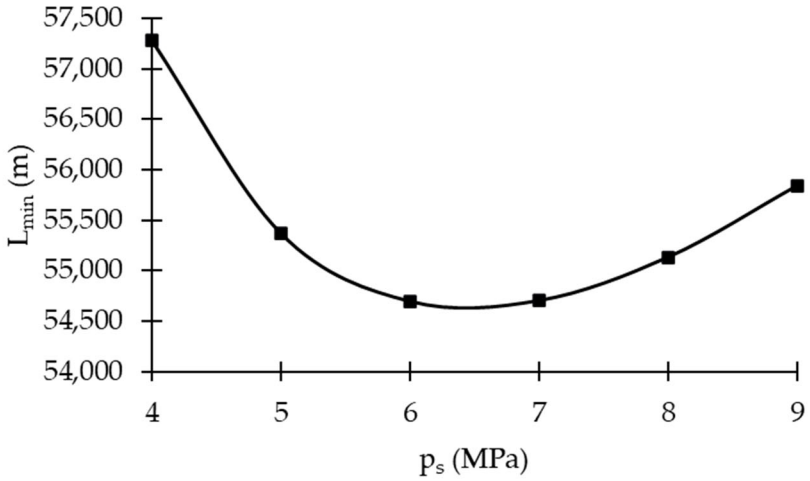

Figure 7. Variation with steam pressure (p_s) of the minimum adjusted total tube length (L_{min}) of the optimized heat recovery steam generator having an individual tube length of 9 m.

By changing l from 7 m to 11 m and keeping p_s at 6.5 MPa, results showing the effects of l were obtained. Table 3 shows that the minimum value of L_{min} is 54,639 m when l is 9 m. However, L_{min} is somewhat insensitive to l in this range. Therefore, the selection of l should be based on other considerations in addition to the total tube material cost.

Table 3. Results of the optimized heat recovery steam generators having 5 different individual tube lengths and operating at 6.5 MPa.

Parameter	Individual Tube Length (l)				
	7 m	**8 m**	**9 m**	**10 m**	**11 m**
N_{c1}	114	103	93	87	77
N_{r1}	10	10	10	10	10
S_{T1}/D_o	1.415	1.402	1.396	1.381	1.391
N_{c2}	97	90	84	77	77
N_{r2}	23	22	21	20	18
S_{T2}/D_o	1.488	1.460	1.438	1.430	1.391
N_{c3}	34	29	26	23	21
N_{r3}	114	114	112	114	116
S_{T3}/D_o	2.392	2.428	2.416	2.441	2.435
m_s (kg/s)	29.01	28.85	28.76	28.60	28.69
T_s (°C)	482.8	487.6	490.3	495.4	492.8
T_{g4} (°C)	175.7	176.4	176.8	177.6	177.2
Δp_g (kPa)	0.398	0.400	0.398	0.401	0.402
L_{min} (m)	54,719	54,648	54,639	54,670	54,747

Since the outer heat transfer coefficient due to gas flow is much less than the inner heat transfer coefficient due to steam or water flow, and the overall heat transfer coefficient increases with the design value of mass flux of gas (G_{gd}), the optimized results are expected to be strongly influenced by G_{gd}. Figure 8 shows that L_{min} decreases linearly as G_{gd} increases. It is, therefore, logical to increase G_{gd} to a higher value. However, there is an upper limit of G_{gd} because higher G_{gd} may result in stronger flow-induced vibration [38]. Furthermore, the risk of tube erosion is higher if the gas contains particulate matter. It is interesting to note that previous studies on thermal-hydraulic models of heat recovery steam generators did not recognize the importance of G_{sd} sufficiently, and placed artificial limits on it [3,4,8,9,12]. These constraints may have resulted in unnecessarily low values of G_{gd}.

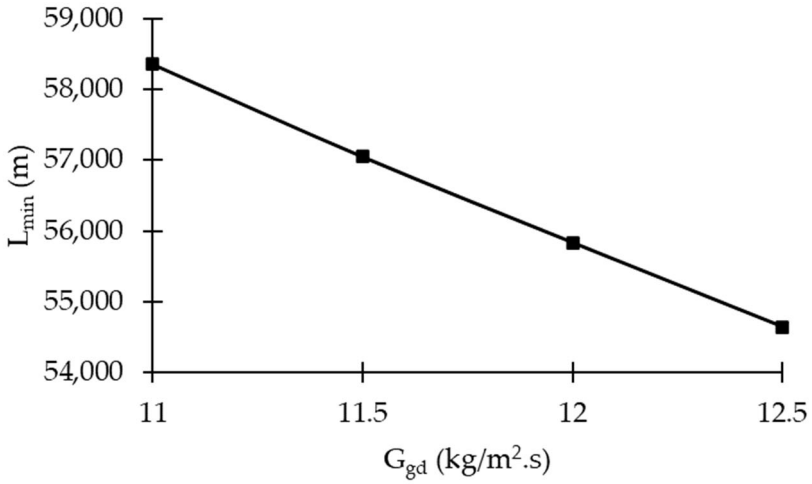

Figure 8. Variation in minimum adjusted total tube length (L_{min}) with the design value of mass flux of gas (G_{gd}).

6. Conclusions

As the heat source in a Rankine cycle, a heat recovery steam generator produces steam using thermal energy from the inlet gas. When the inlet gas contains a significant amount of particulate matter, the heat recovery steam generator should use bare or finless tubes.

Components of a heat recovery steam generator are a superheater, an evaporator, and an economizer. They are cross-flow heat exchangers consisting of inline tube banks. The configuration of a tube bank is characterized by the tube diameters, the number of tube columns, the number of tube rows, the tube pitches, and the individual tube length, which are known as geometric parameters. The individual tube length represents the size of the heat recovery steam generator. The objective of this paper is to demonstrate that there is an optimal geometric configuration under specified conditions. Based on the specified value of net power output in the Rankine cycle in which the heat recovery steam generator is the heat source and the specified size of the heat recovery steam generator, the optimal geometric parameters of the superheater, evaporator, and economizer can be determined that result in the minimum tube material cost. For the case study of a system in which the inlet gas flow rate and temperature are 200 kg/s and 580 °C, the individual tube length is 9 m, the net power output is 30 MW, and the maximum mass flux of gas is 12.5 kg/m^2.s; the minimum adjusted total tube length of the optimized heat recovery steam generator is 54,639 m. The optimal numbers of tube columns in the superheater, evaporator, and economizer are 93, 84, and 26. The optimal numbers of tube rows in the superheater, evaporator, and economizer are 10, 21, and 112. The mass flow rate, pressure, and temperature of the steam produced by the optimized heat recovery steam generator are 29.76 kg/s, 6.5 MPa, and 490.3 °C. The minimum adjusted total tube length is relatively insensitive to the individual tube length in the range between 7 m and 11 m.

Funding: This research received no external funding.

Data Availability Statement: The raw data supporting the conclusions of this article will be made available by the authors on request.

Conflicts of Interest: The author declares no conflicts of interest.

Abbreviations

Nomenclature

A	Heating surface area of heat exchanger, m^2
C	Capacity rate, W/°C
c	Ratio of capacity rates
D	Tube diameter, m
f	Friction factor
ff	Fouling factor, m^2.K/W
G	Mass flux, kg/m^2.s
h	Enthalpy, kJ/kg
$\overline{h}$	Heat transfer coefficient, kW/m^2.°C
K	Minor loss coefficient
k	Thermal conductivity, kW/m.°C
l	Individual tube length, m
m	Mass flow rate, kg/s
N	Number of tubes
NTU	Number of transfer units
P	Power, MW
p	Pressure, kPa
Pr	Prandtl number
r	Ratio of unit costs of low alloy steel tube and carbon steel tube
Re	Reynolds number
S	Tube pitch, m
T	Temperature, °C
U	Overall heat transfer coefficient, kW/m^2.°C
V	Velocity, m/s
v	Specific volume, m^3/kg

Greek Symbols	
ε	Effectiveness of heat exchanger
η	Efficiency
μ	Dynamic viscosity, Pa.s
ρ	Density, kg/m^3
Subscripts	
atot	Adjusted total
e	Exit
c	Condenser, tube column
EC	Economizer
EV	Evaporator
g	Gas
i	Inlet, inner tube surface
L	Longitudinal
l	Saturated liquid
o	Outer tube surface
r	Tube row
s	Steam
sat	Saturated
T	Transverse
v	Saturated steam
w	Liquid water

References

1. Valdes, M.; Duran, M.D.; Rovira, A. Thermoeconomic optimization of combined cycle gas turbine power plants using genetic algorithms. *Appl. Therm. Eng.* **2003**, *23*, 2169–2182. [CrossRef]
2. Franco, A.; Giannini, N. A general method for the optimum design of heat recovery steam generators. *Energy* **2006**, *31*, 3342–3361. [CrossRef]
3. Manassaldi, J.I.; Mussati, S.F.; Scenna, N.J. Optimal synthesis and design of Heat Recovery Steam Generation (HRSG) via mathematical programming. *Energy* **2011**, *36*, 475–485. [CrossRef]
4. Norouzi, E.; Mehrgoo, M.; Amidpour, M. Geometric and thermodynamic optimization of a heat recovery steam generator: A constructal design. *J. Heat Trans.* **2012**, *134*, 111801. [CrossRef]
5. Duran, M.D.; Valdes, M.; Rovira, A.; Rincon, E. A methodology for the geometric design of heat recovery steam generators applying genetic algorithms. *Appl. Therm. Eng.* **2013**, *52*, 77–83. [CrossRef]
6. Esmaieli, A.; Keshavarz, M.P.; Shakib, S.E.; Amidpour, M. Applying different optimization approaches to achieve optimal configuration of a dual pressure heat recovery steam generator. *Int. J. Energy Res.* **2013**, *37*, 1440–1452. [CrossRef]
7. Sharma, M.; Singh, O. Parametric evaluation of heat recovery steam generator (HRSG). *Heat Trans. Asian Res.* **2014**, *43*, 691–705. [CrossRef]
8. Mehrgoo, M.; Amidpour, M. Constructal design and optimization of a dual pressure heat recovery steam generator. *Energy* **2017**, *124*, 87–99. [CrossRef]
9. Mehrgoo, M.; Amidpour, M. Configurations and pressure levels optimization of heat recovery steam generator using the genetic algorithm method based on the constructal design. *Appl. Therm. Eng.* **2017**, *122*, 601–617. [CrossRef]
10. Ahmed, A.; Esmaeil, K.K.; Irfan, M.A.; Al-Mufadi, F.A. Design methodology of heat recovery steam generator in electric utility for waste heat recovery. *Int. J. Low-Carbon Technol.* **2018**, *13*, 369–379. [CrossRef]
11. Rezaie, A.; Tsatsaronis, G.; Hellwig, U. Thermal design and optimization of a heat recovery steam generator in a combined-cycle power plant by applying a genetic algorithm. *Energy* **2019**, *168*, 346–357. [CrossRef]
12. Norouzi, E.; Amidpour, M.; Rezakazemi, M. Heat recovery steam generator: Constructal thermoeconomic optimization. *Appl. Therm. Eng.* **2019**, *148*, 747–753. [CrossRef]
13. Ghaffari, A.; Ahmadi, R.; Eyvazkhani, M. Modeling and optimization of finless and finned tube heat recovery steam generators for cogeneration plants. *Eng. Rep.* **2020**, *2*, 12262. [CrossRef]
14. Mohtaram, S.; Sun, Y.; Sun, H.; Abrishami, A.; Omidi, M.; Lin, J. A comprehensive design, optimization and development methodology of a wasted heat recovery boiler using serrated fins and extensive surface in a bulky CCPP. *Case Stud. Therm. Eng.* **2021**, *23*, 100808. [CrossRef]
15. Bianco, N.; Fragnito, A.; Iasiello, M.; Mauro, G.M. A comprehensive approach for the multi-objective optimization of heat recovery steam generators to maximize cost-effectiveness and output power. *Sustain. Energy Technol. Assess.* **2021**, *45*, 101162. [CrossRef]

16. Mehrgoo, M.; Amidpour, M. Multiscale structural optimization of dual-pressure heat recovery steam generators using constructal theory. *Int. Comm. Heat Mass Trans.* **2025**, *161*, 108546. [CrossRef]
17. Mehrgoo, M.; Amidpour, M. A constructal theory framework for optimizing HRSG design: Enhancing thermal performance and cost-effectiveness. *Results Eng.* **2025**, *27*, 105849. [CrossRef]
18. Tong, S.; Chen, X.; Tong, Z.; Yang, Q. Numerical design and optimization of finned tube heat exchanger with curved serration based on multi-layered neural network and tree-structured Parzen estimator algorithm. *J. Therm. Sci.* **2025**, *34*, 1417–1430. [CrossRef]
19. Erguvan, M.; MacPhee, D.W. Second law optimization of heat exchangers in waste heat recovery. *Int. J. Energy Res.* **2019**, *43*, 5714–5734. [CrossRef]
20. Kuru, M.N.; Ozkarakoç, M.; Erdinç, M.T.; Karasu, I.; Ünal, S. Optimized tube bank configurations: A multi-objective approach to entropy and volume minimization. *Appl. Therm. Eng.* **2025**, *278*, 127003. [CrossRef]
21. Khan, M.N.; Tlili, I. Innovative thermodynamic parametric investigation of gas and steam bottoming cycles with heat exchanger and heat recovery steam generator: Energy and exergy analysis. *Energy Rep.* **2018**, *4*, 497–506. [CrossRef]
22. Najjar, Y.S.H.; Alalul, O.F.A.; Abu-Shamleh, A. Degradation analysis of a combined cycle heat recovery steam generator under full and part load conditions. *Sustain. Energy Technol. Assess.* **2020**, *37*, 100587. [CrossRef]
23. In, J.S.; Lee, S.Y. Optimization of heat recovery steam generator through exergy analysis for combined cycle gas turbine power plants. *Int. J. Energy Res.* **2008**, *32*, 859–869. [CrossRef]
24. Godoy, E.; Scenna, N.J.; Benz, S.J. Families of optimal thermodynamic solutions for combined cycle gas turbine (CCGT) power plants. *Appl. Therm. Eng.* **2010**, *30*, 569–576. [CrossRef]
25. Bracco, S.; Siri, S. Exergetic optimization of single level combined gas-steam power plants considering different objective functions. *Energy* **2010**, *35*, 5365–5373. [CrossRef]
26. Nadir, M.; Ghenaiet, A.; Carcasci, C. Thermo-economic optimization of heat recovery steam generator for a range of gas turbine exhaust temperatures. *Appl. Therm. Eng.* **2016**, *106*, 811–826. [CrossRef]
27. Almajali, M.R.; Quran, O.A.S. Parametric study on the performance of combined power plant of steam and gas turbines. *J. Therm. Sci. Eng. Applic.* **2021**, *13*, 051006. [CrossRef]
28. Li, B.; Deng, Y.; Li, Z.; Xu, J.; Wang, H. Thermal-economy optimization for single/dual/triple-pressure HRSG of gas-steam combined cycle by multi-objective genetic algorithm. *Energy Convers. Manag.* **2022**, *258*, 115471. [CrossRef]
29. Zolfigol, A.; Salehi, G.; Nimafar, M.; Khams, A.A. Simulation and 4E analysis of combined cycle with single, dual, and triple pressure heat recovery steam generators integrated with organic Rankine cycle and solar energy. *Results Eng.* **2026**, *29*, 108585. [CrossRef]
30. Dhar, P.L. *Thermal System Design and Simulation*; Elsevier: Amsterdam, The Netherlands, 2017.
31. Chen, N.H. An explicit equation for friction factors in pipes. *Ind. Eng. Chem. Funda.* **1979**, *18*, 296–297. [CrossRef]
32. Gnielinski, V. New equations for heat and mass transfer in turbulent pipe and channel flow. *Int. Chem. Eng.* **1976**, *16*, 359–368.
33. Ganapathy, V. *Steam Generators and Waste Heat Boilers for Process and Plant Engineers*; CRC Press: Boca Raton, FL, USA, 2015.
34. NIST Chemistry WebBook. Available online: https://webbook.nist.gov/chemistry (accessed on 15 October 2026).
35. Wagner, W.; Cooper, J.R.; Dittmann, A.; Kijima, J.; Kretzschmar, H.J.; Kruse, A.; Mareš, R.; Oguchi, K.; Sato, H.; Stöcker, I.; et al. The IAPWS industrial formulation 1997 for the thermodynamic properties of water and steam. *J. Eng. Gas Turb. Power* **2000**, *122*, 150–180. [CrossRef]
36. Sengers, J.V.; Kamgar-Parsi, B. Representative equations for the viscosity of water substance. *J. Phys. Chem. Ref. Data* **1984**, *13*, 185–205. [CrossRef]
37. Sengers, J.V.; Watson, J.T.R.; Basu, R.S.; Kamgar-Parsi, B.; Hendricks, R.C. Representative equations for the thermal conductivity of water substance. *J. Phys. Chem. Ref. Data* **1984**, *13*, 893–933. [CrossRef]
38. Deng, H.; Skaugen, G.; Næss, E.; Zhang, M.; Øiseth, O.A. A novel methodology for design optimization of heat recovery steam generators with flow-induced vibration analysis. *Energy* **2021**, *226*, 120325. [CrossRef]

Disclaimer/Publisher's Note: The statements, opinions and data contained in all publications are solely those of the individual author(s) and contributor(s) and not of MDPI and/or the editor(s). MDPI and/or the editor(s) disclaim responsibility for any injury to people or property resulting from any ideas, methods, instructions or products referred to in the content.